

Nonlinear stability and bifurcations of an axially accelerating beam with an intermediate spring-support

Mergen H. Ghayesh* and Marco Amabili

Department of Mechanical Engineering, McGill University, Montreal, Quebec, Canada H3A 0C3

(Received May 12, 2013, Revised June 26, 2013, Accepted July 11, 2013)

Abstract. The present work aims at investigating the nonlinear dynamics, bifurcations, and stability of an axially accelerating beam with an intermediate spring-support. The problem of a parametrically excited system is addressed for the gyroscopic system. A geometric nonlinearity due to mid-plane stretching is considered and Hamilton's principle is employed to derive the nonlinear equation of motion. The equation is then reduced into a set of nonlinear ordinary differential equations with coupled terms via Galerkin's method. For the system in the sub-critical speed regime, the pseudo-arclength continuation technique is employed to plot the frequency-response curves. The results are presented for the system with and without a three-to-one internal resonance between the first two transverse modes. Also, the global dynamics of the system is investigated using direct time integration of the discretized equations. The mean axial speed and the amplitude of speed variations are varied as the bifurcation parameters and the bifurcation diagrams of Poincare maps are constructed.

Keywords: axially moving beams; nonlinear dynamics; additional spring-support

1. Introduction

Beam structures (Ghayesh *et al.* 2011, Sahebkar *et al.* 2011, Kural and Özkaya 2012, Movahedian 2012, Saffari *et al.* 2012, Song *et al.* 2012, Bayat *et al.* 2013) are present in many engineering devices and machine components. Among them, robot arms, aerial cable tramways, textile fibers, automobile and aerospace structures, conveyor belts, magnetic tapes, and fluid-conveying pipes can be modeled as axially moving beams (Ravindra and Zhu 1988, Ding and Chen 2009, Chen *et al.* 2012, Ghayesh *et al.* 2013). These widespread applications have stimulated continuing research on this topic, as evident from literature.

The axial speed greatly affects the dynamical behavior of axially moving systems by producing travelling waves and centrifugal forces. Real-life axially moving systems do not travel at a constant axial speed, mainly due to some internal or external imperfections; there are always some small variations in the axial speed over the mean value. Therefore, the axial speed can be modelled by superimposing some harmonic fluctuations in time on the mean value to obtain an axial acceleration. This time-variant variation in the axial speed is very important since it can cause

* Corresponding author, Ph.D., E-mail: mergen.hajghayesh@mail.mcgill.ca

parametric resonances.

The literature concerning the dynamics of axially moving beams and strings undergoing a *constant* axial speed is quite large. Such examples are the following papers: Marynowski and Kapitaniak (2002) who employed two different energy dissipation mechanism in the model of an axially moving web. Ding and Chen (2010) determined the nonlinear natural frequencies of high-speed axially moving beams using the Galerkin method. Huang *et al.* (2011) examined the forced sub-critical dynamics of an axially moving beam via harmonic balance method. Pellicano and Vestroni (2000) examined the dynamics of an axially moving beam in both the sub- and super-critical speed regimes. Tang *et al.* (2008) determined the natural frequencies, mode functions, and critical speeds of an axially moving Timoshenko beam. Riedel and Tan (2002) employed the method of multiple timescales and the Galerkin technique to examine the coupled vibrations of an axially moving beam. Ghayesh (2011) studied the nonlinear dynamics of an axially moving viscoelastic beam with an internal resonance. Ghayesh (2011) determined the natural frequencies, mode functions, and critical speeds of an axially moving laminated composite beam.

The dynamics of an axially *accelerating* beam or string has been investigated for many years by various authors (Pakdemirli *et al.* 1994, Parkdemirli and Ulsoy 1997, Öz and Pakdemirli 1999, Özkaya and Pakdemirli 2000, Suweken and Van 2003, Pakdemirli 2008, Sahebkar *et al.* 2011). Most of these studies (Pakdemirli *et al.* 1994, Parkdemirli and Ulsoy 1997, Öz *et al.* 1998, Öz and Pakdemirli 1999, Özkaya and Pakdemirli 2000, Öz *et al.* 2001, Ghayesh 2008, Ghayesh and Balar 2010, Sahebkar *et al.* 2011) employed analytical techniques, mainly the method of multiple timescales so as to determine the single-mode approximation for the resonant response of the system. For example, Oz and Pakdemirli (1999) investigated the linear parametric vibrations and stability of an axially accelerating beam via the method of multiple timescales. In a series of papers, a systematic research on this topic was conducted by Ghayesh and co-workers (Ghayesh and Khadem 2007, Ghayesh 2008, Ghayesh and Balar 2008, Ghayesh 2009, 2010, Ghayesh and Balar 2010, Ghayesh *et al.* 2010) including several system models such as linear, nonlinear, energy dissipative, Euler-Bernoulli, Rayleigh, Timoshenko, and laminated composite models. There are also some other works in the literature which considered direct time integration of discretized equations of motion to examine the global dynamics of the system (Yang and Chen 2005). The current paper addresses the lack of research on the sub-critical resonant response of an axially moving beam via efficient numerical technique, and employing larger degrees of freedom in discretization. Moreover, the global dynamics of the system is investigated via direct time integration of discretized equations.

In some applications, beams are subject to *intermediate concentrated elements* such as point masses and springs. The vibrations and stability of *stationary* (not traveling) beams with intermediate elements have received considerable attention in the literature. The literature regarding the dynamics of axially moving systems with intermediate elements, on the other hand, is not large. For instance, the stability characteristics of an axially accelerating string supported by a partial elastic foundation were examined via the method of multiple scales by Ghayesh (2009). This paper addresses an axially moving beam with an intermediate spring-support which can be simplified model of an intermediate support in real mechanical systems.

In the present paper, the nonlinear dynamics, bifurcations, and stability of an axially accelerating beam with an intermediate spring-support are examined numerically. The equation of motion is derived via Hamilton's method and discretized using the Galerkin method, yielding a set of nonlinear ordinary differential equations with time-dependent coefficients and coupled terms.

The sub-critical resonant response is obtained via the pseudo-arclength continuation technique for the system when possessing a three-to-one internal resonance and when it is not. The bifurcation diagrams of Poincare maps for this parametrically excited system are also constructed via direct time integration. The results are presented in the form of time histories, phase-plane diagrams, Poincare maps, and fast Fourier transforms (FFTs).

2. Problem statement, equation of motion, and methods of solution

Shown schematically in Fig.1 is a hinged-hinged axially accelerating beam of length L , with cross-sectional area A , constant density ρ , area moment of inertia I , and Young's modulus E , which is traveling at a time-dependent axial speed $V(t)$. Moreover, the beam is subjected to a pretension p , and a spring with linear and nonlinear stiffness coefficients of k_1 and k_2 respectively, which is attached at a distance \hat{x}_s from the left end of the beam.

The equation of motion for a hinged-hinged axially accelerating beam additionally supported by a nonlinear spring is derived in the following via Hamilton's principle under the assumptions : (i) only the transverse displacement is considered (Pakdemirli *et al.* 1994, Suweken and Van 2003, Marynowski 2004, Chen and Yang 2005, Ahmadian *et al.* 2010) (ii) the beam has a uniform cross-sectional area; (iii) the beam is modelled via nonlinear Euler-Bernoulli beam theory; (iv) the type of nonlinearity is geometric and comes from the stretching effect of the mid-plane of the beam; (v) the equation of motion is truncated at third order; (vi) the nonlinear spring is assumed to be attached to the centerline of the beam and the force generated by is assumed to be purely in the transverse direction; (vii) the axial speed is assumed to involve a constant mean value along with a term which is harmonic function of time.

The potential energy of the system is given by

$$\pi = \frac{1}{2}EA \int_0^L \left[\frac{1}{2} \left(\frac{\partial w}{\partial x} \right)^2 \right]^2 dx + \frac{1}{2}EI \int_0^L \left(\frac{\partial^2 w}{\partial x^2} \right)^2 dx + p \int_0^L \left[\frac{1}{2} \left(\frac{\partial \hat{w}}{\partial \hat{x}} \right)^2 \right] dx + \int_0^L \left(\frac{1}{2}k_1 w^2 + \frac{1}{4}k_2 w^2 \right) \delta(x - x_s) dx \quad (1)$$

where $w(x,t)$ represents the transverse displacement and $\delta(x)$ is the Dirac delta function. In Eq. (1), the first term on the right-hand side is due to the mid-plane stretching, the second term is due to the flexural restoring force, the third to the pretension, and the last one to the spring force acting on the beam.

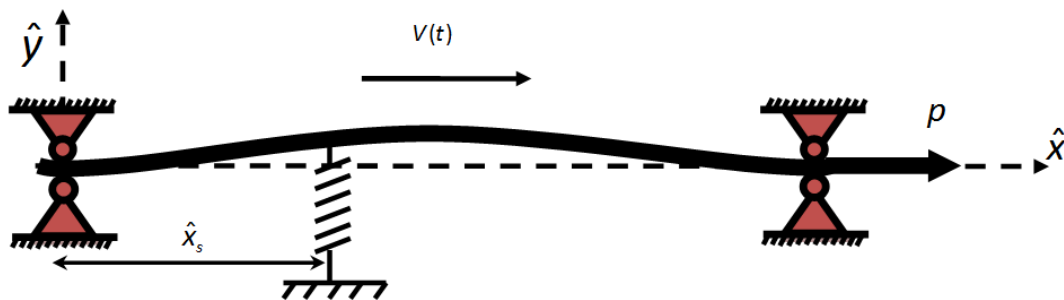


Fig. 1 Schematic representation of an axially accelerating beam with an intermediate spring-support

The kinetic energy of the system is given by

$$T = \frac{1}{2} \rho A \int_0^L [V(t)]^2 dx + \frac{1}{2} \rho A \int_0^L \left[\frac{\partial w}{\partial t} + V(t) \frac{\partial w}{\partial \hat{x}} \right]^2 dx \quad (2)$$

The kinetic and potential energies of the system (Eqs. (1) and (2)) can all be combined via Hamilton's principle. This operation yields the following dimensionless equation of motion

$$\frac{\partial^2 w}{\partial \tau^2} + 2v \frac{\partial^2 w}{\partial x \partial \tau} + \frac{dv}{d\tau} \frac{\partial w}{\partial x} + (v^2 - 1) \frac{\partial^2 w}{\partial x^2} + v_f^2 \frac{\partial^4 w}{\partial x^4} + \delta(x - x_s)(\partial w + \gamma w^3) = \frac{3}{2} v_1^2 \frac{\partial^2 w}{\partial x^2} \left(\frac{\partial w}{\partial x} \right)^2 \quad (3)$$

where the dimensionless parameters are defined as

$$x = \frac{x}{L}, \quad x_s = \frac{\hat{x}_s}{L}, \quad w = \frac{w}{L}, \quad \tau = t \sqrt{\frac{p}{\rho A L^2}}, \quad v = V \sqrt{\frac{\rho A}{p}} \quad (4)$$

$$v_1 = \sqrt{\frac{EA}{p}}, \quad v_f = \sqrt{\frac{EI}{pL^2}}, \quad \alpha = \frac{k_1 L}{p}, \quad \gamma = \frac{k_2 L^3}{p}$$

The dimensionless equations for boundary conditions of a hinged-hinged beam are given by

$$w|_{x=0} = \frac{\partial^2 w}{\partial x^2} \Big|_{x=0} = 0, \quad w|_{x=1} = \frac{\partial^2 w}{\partial x^2} \Big|_{x=1} = 0 \quad (5)$$

The axial speed is assumed to involve a constant mean value f_0 along with a harmonic fluctuations, $f_1 \sin(\Omega\tau)$, where Ω and f_1 represent the frequency and the amplitude of the speed variations respectively.

Employing the well-known Galerkin method on Eq. (3) in order to discretized this equation results in

$$\begin{aligned} & \sum_{j=1}^N \left(\int_0^1 \phi_i \phi_j dx \right) \dot{q}_j + 2(f_0 + f_1 \sin(\Omega\tau)) \sum_{j=1}^N \left(\int_0^1 \phi_i \phi_j' dx \right) \dot{q}_j + f_1 \Omega \cos(\Omega\tau) \sum_{j=1}^N \left(\int_0^1 \phi_i \phi_j' dx \right) \dot{q}_j \\ & + (f_0^2 - 1 + f_1^2 \sin^2(\Omega\tau) + 2f_0 f_1 \sin(\Omega\tau)) \sum_{j=1}^N \left(\int_0^1 \phi_i \phi_j'' dx \right) q_j + v_f^2 \sum_{j=1}^N \left(\int_0^1 \phi_i \phi_j''' dx \right) q_j \\ & + \alpha \sum_{j=1}^N \left(\int_0^1 \delta(x - x_s) \phi_i \phi_j dx \right) q_j + \gamma \sum_{j=1}^N \sum_{k=1}^N \sum_{l=1}^N \left(\int_0^1 \delta(x - x_s) \phi_i \phi_j \phi_k \phi_l dx \right) q_j q_k q_l \\ & = \frac{3}{2} v_1^2 \sum_{j=1}^N \sum_{k=1}^N \sum_{l=1}^N \left(\int_0^1 \phi_i \phi_j'' \phi_k' \phi_l' dx \right) q_j q_k q_l \quad i = 1, 2, \dots, N \end{aligned} \quad (6)$$

where $\phi_i(x) = \sin(i\pi x)$ denotes the i^{th} eigenfunction of a hinged-hinged beam and $q_i(\tau)$ represents the i^{th} generalized coordinate. The dot and prime superscripts represent the differentiation with respect to dimensionless time and axial coordinate respectively.

Eq. (6) forms a set of N ordinary differential equations with coupled non-inertial terms. Transforming this set via $y_i = \dot{q}_i$ for $i=1, 2, \dots, N$ doubles the number of equations to $2N$, but allows us to utilize standard numerical techniques; most numerical techniques can best handle first

order ordinary differential equations rather than second-order ones. Twelve first-order ordinary differential equations are solved in this paper employing two different numerical techniques. The first technique uses the pseudo-arclength continuation technique to obtain frequency-response curves of the system (Doedels *et al.* 1998). In the second technique, the variable step-size Runge-Kutta method is employed to the direct time integration (Ghayesh and Païdoussis 2010, Ghayesh *et al.* 2011, Ghayesh 2012, Ghayesh *et al.* 2012) of Eq. (6) and to construct the bifurcation diagrams of Poincare maps. Although there is no damping term in the equation of motion, the numerical analyses include viscous damping μ .

3. Frequency-response curves of the system in the sub-critical speed regime

The frequency-response curves of the system away from internal resonances between the first two modes as well as the case possessing a three-to-one internal resonance between the first two modes are plotted in this section. For the case with an internal resonance, the curves are plotted for two values of the excitation amplitude. As we shall see, the frequency-response curves typically show a trivial solution, both stable and unstable, throughout the solution space separated by bifurcation points. All the results of this section were obtained using the pseudo-arclength continuation technique.

3.1 Parametric response of the system with no internal resonances between the first two modes

In this section the nonlinear parametric response of the system without any internal resonances between the first two modes is examined. The following dimensionless parameters have been selected in the analysis of this section: $\nu_1=33.526$, $\nu_f=0.173$, $\mu=0.05$, $f_0=0.3$, $f_1=0.08$, $\alpha=3.0$, $\gamma=0.5$,

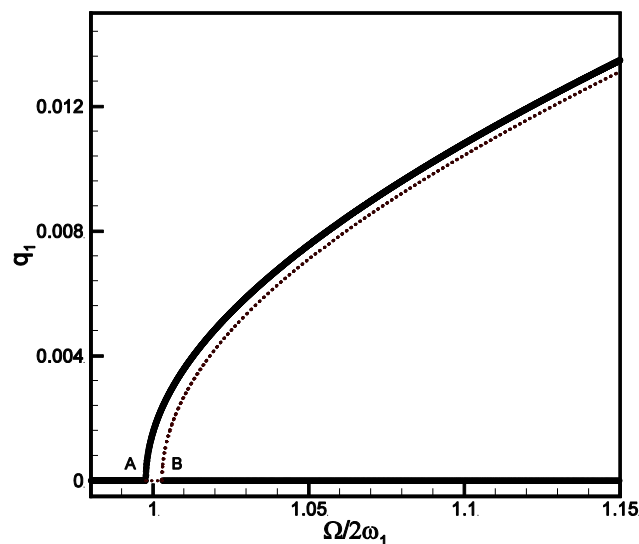


Fig. 2 The frequency-response curve of the system with no internal resonances between the first two modes. Bold line and dotted lines represent the stable and unstable solutions respectively

and $x_s=0.5$; the spring is located at the mid-point of the beam. As seen in Fig. 2, it was found that as the excitation frequency is increased gradually from $\Omega=0.98\times 2\omega_1$ (i.e., the resonance occurs when the excitation frequency approaches *twice the amount of* any linear natural frequency of the system), the amplitude of the first generalized coordinate remains zero until the first period-doubling bifurcation occurs at point A ($\Omega=0.9976\times 2\omega_1$) where the trivial solution loses stability, and a stable non-trivial solution branch bifurcates. The amplitude of this stable non-trivial solution increases with the excitation frequency until $\Omega=1.1500\times 2\omega_1$. The trivial solution branch regains the stability at point B ($\Omega=1.0028\times 2\omega_1$) via the second period-doubling bifurcation point. At this point, unstable non-trivial solution branch also bifurcates; the amplitude of this branch increases with the excitation frequency until $\Omega=1.1500\times 2\omega_1$.

3.2 Parametric response of the system possessing a three-to-one internal resonance between the first two modes

In this section, the parametric resonant response of the system possessing a three-to-one internal resonance is investigated for two cases with different excitation amplitudes. This is accomplished by carefully selecting system parameters such that: $\nu_1=33.526$, $\nu_2=0.173$, $\mu=0.05$, $f_0=0.702$, $\alpha=3.5$, $\gamma=0.7$, and $x_s=0.2$ which yields the second linear natural frequency of the system to be approximately three times that of the first one. Two cases are addressed in the following; in the first case the excitation amplitude is set to $f_1=0.08$ and in the second case to a smaller value of $f_1=0.05$.

3.2.1 Case 1: Parametric response of the system having a three-to-one internal resonance between the first two modes with $f_1=0.08$

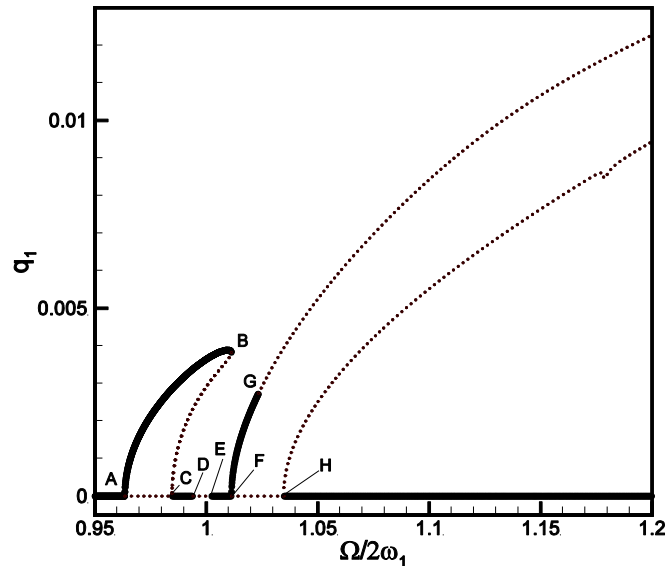


Fig. 3 The frequency-response curve of the system, associated with Case 1 with $f_1=0.08$, possessing a three-to-one internal resonance between the first two modes. Bold line and dotted lines represent the stable and unstable solutions respectively

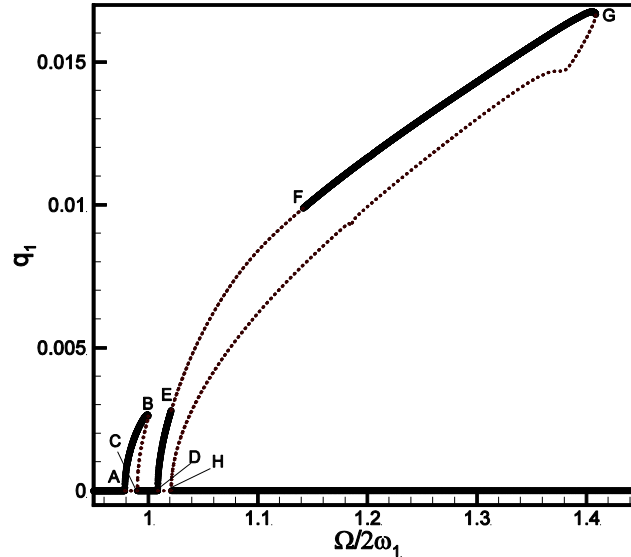


Fig. 4 The frequency-response curve of the system, associated with Case 2 with $f_1=0.05$ possessing a three-to-one internal resonance between the first two modes. Bold line and dotted lines represent the stable and unstable solutions respectively

Fig. 3 shows that as the excitation frequency is increased gradually from $\Omega=0.95 \times 2\omega_1$, there is only one stable trivial solution until point A ($\Omega=0.9634 \times 2\omega_1$) where a stable non-trivial solution bifurcates and the trivial solution loses stability. As the excitation frequency is increased further, the amplitude of the stable non-trivial solution increases accordingly until it reaches a limit point bifurcation at B ($\Omega=1.0112 \times 2\omega_1$) where it becomes unstable. The amplitude of this now unstable non-trivial branch decreases until point C ($\Omega=0.9845 \times 2\omega_1$) is hit, where the trivial solution regains the stability via a period-doubling bifurcation. This stability is lost again at point D ($\Omega=0.9940 \times 2\omega_1$) via the first torus bifurcation and retrieved at point E ($\Omega=1.0022 \times 2\omega_1$) via the second torus bifurcation. As the excitation frequency is increased even further, another period-doubling bifurcation occurs at F ($\Omega=1.0113 \times 2\omega_1$). At this point, the trivial solution loses stability and a stable non-trivial solution bifurcates, which loses stability at Point G ($\Omega=1.0232 \times 2\omega_1$) via a torus bifurcation. This unstable non-trivial solution branch continues until $\Omega=1.2000 \times 2\omega_1$. There is also another period-doubling bifurcation point at H where $\Omega=1.0346 \times 2\omega_1$.

3.2.2 Case 2: Parametric response of the system having a three-to-one internal resonance between the first two modes with $f_1=0.05$

Decreasing the excitation amplitude from 0.08 to 0.05 in Figs. 3 and 4 is generated. As seen in this figure, there are five trivial solution branches, three stable and two unstable, six non-trivial solution branches, three stable and three unstable. In other words, as the excitation frequency is increased gradually from $\Omega=0.95 \times 2\omega_1$, the amplitude of the first generalized coordinate, remains zero until the first period-doubling bifurcation point at A ($\Omega=0.9785 \times 2\omega_1$) is hit, where the stability of the trivial solution is lost and a stable non-trivial solution bifurcates. The amplitude of the stable non-trivial solution increases with Ω until point B ($\Omega=0.9998 \times 2\omega_1$) where a limit point

bifurcation occurs. The second period-doubling bifurcation occurs at point C ($\Omega=0.9899\times 2\omega_1$), where the trivial solution regains the stability.

As the excitation frequency is increased further, the third period-doubling bifurcation occurs at point D ($\Omega=1.0086\times 2\omega_1$), where the trivial solution loses stability and a stable non-trivial solution bifurcates, which loses stability at E ($\Omega=1.0208\times 2\omega_1$) via a torus bifurcation and regains it via reverse torus bifurcation at point F ($\Omega=1.1413\times 2\omega_1$). The amplitude of this now stable non-trivial solution increases with the excitation frequency until a limit point bifurcation at point G ($\Omega=1.4083\times 2\omega_1$) is reached. At this point, the stability is lost once again. Decreasing the excitation frequency, the amplitude of the unstable non-trivial solution decreases until the last period-doubling bifurcation at point H ($\Omega=1.0207\times 2\omega_1$) is hit. At this point, the stability of the trivial solution is regained.

4. Complex nonlinear dynamics of the system

The bifurcation diagrams of Poincaré maps of the system, obtained from direct time integration of the transformed form of Eq. (6) using the variable step-size Runge-Kutta method, are presented in this section. Although the AUTO code is capable of providing continuation of solutions and stability and bifurcation analysis, it cannot obtain quasiperiodic and chaotic motions. The mean axial speed and the amplitude of the axial speed variations are chosen as bifurcation parameters. The computations were carried out for a time interval of [0 2500] dimensionless seconds and the last 30% of the time response is taken as steady state responses. The phase-space is sectioned in every period of the speed fluctuations and the Poincaré maps are plotted versus the bifurcation parameter. The state of the system at each step is adopted as the initial conditions for the next step. In this section it is implied that the *response* and *amplitude* are with respect to the q_1 motion where it is sectioned, respectively.

4.1 The mean axial speed as the bifurcation parameter

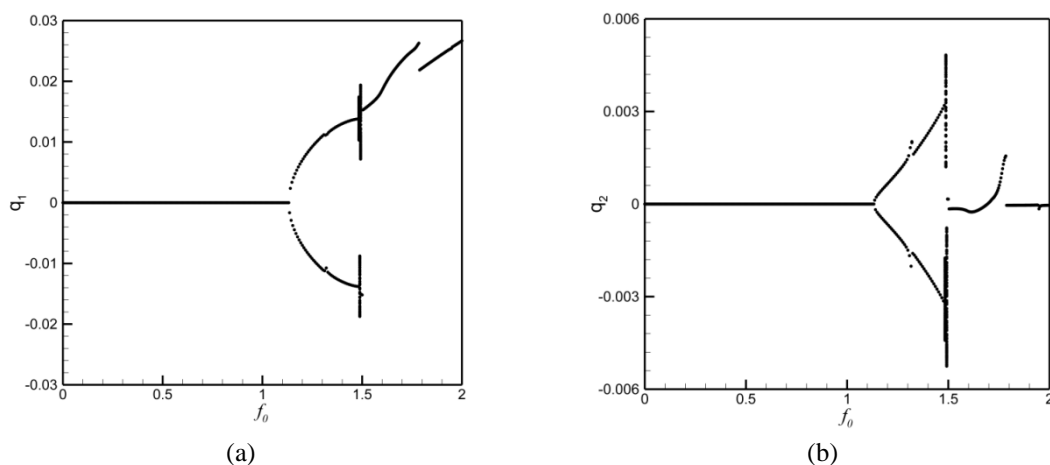


Fig. 5 Bifurcation diagrams of Poincaré points for increasing mean axial speed of the system with $f_1=0.05$

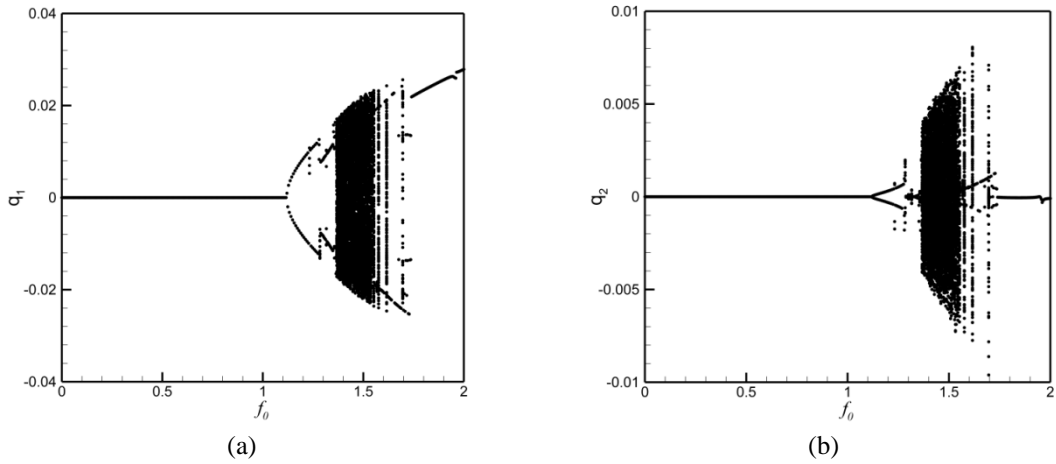


Fig. 6 Bifurcation diagrams of Poincaré points for increasing mean axial speed of the system with $f_1=0.1$

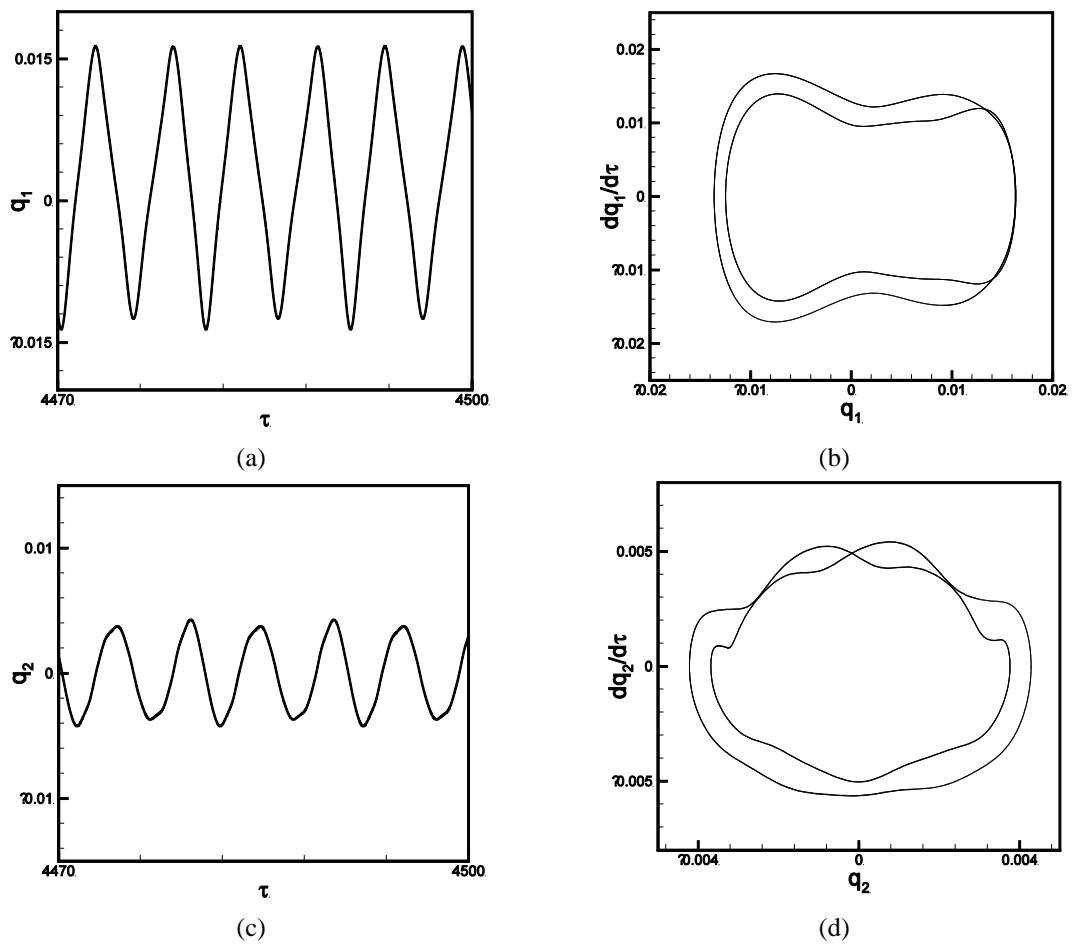


Fig.7 Period-2 oscillation for the system of Fig. 6 at $f_0=1.36$; (a), (b) time trace and phase-plane portrait of the q_1 motion respectively; (c), (d) time trace and phase-plane portrait of the q_2 motion respectively

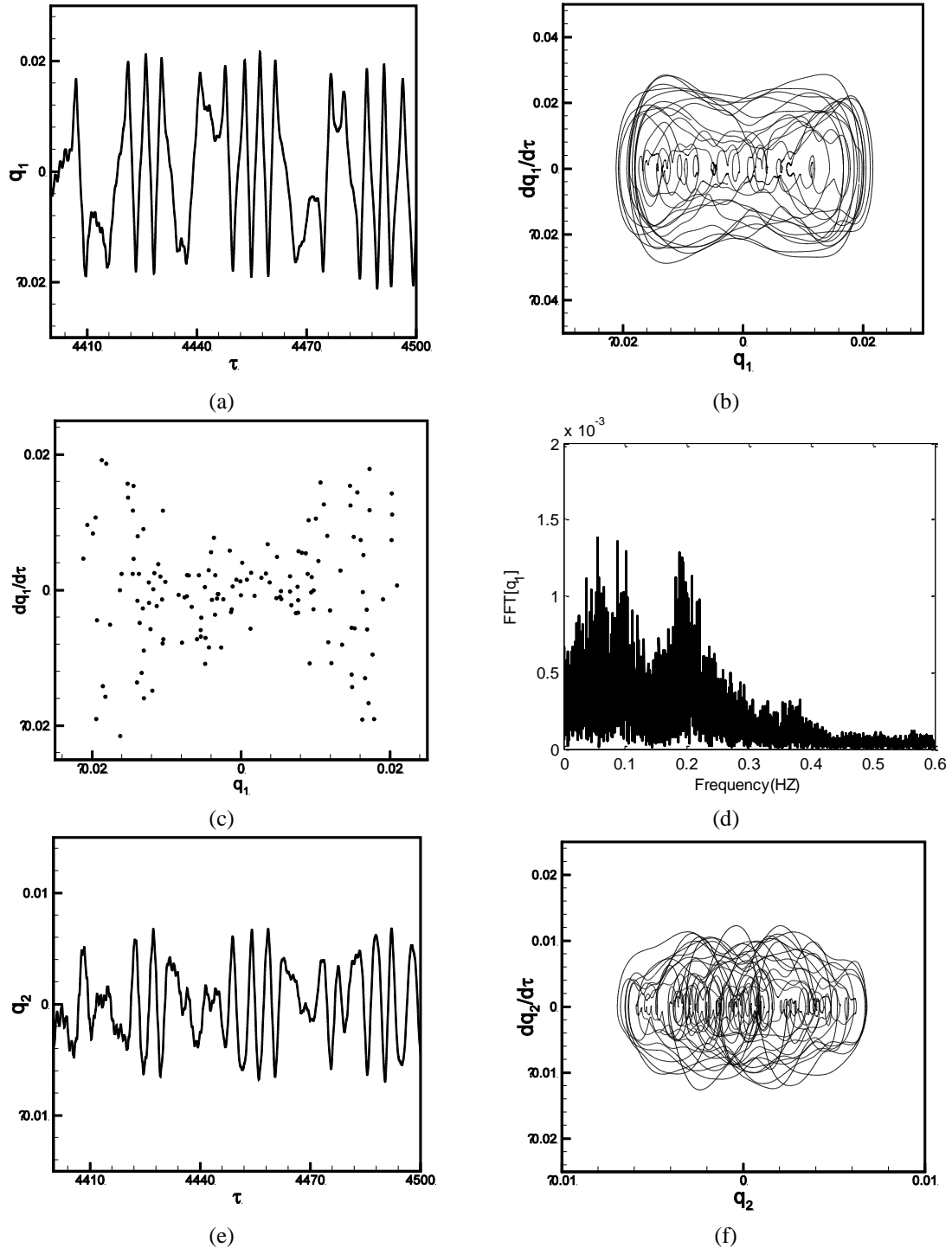


Fig. 8 Chaotic oscillation for the system of Fig. 6 at $f_0=1.48$; (a), (b) time trace and phase-plane portrait of the q_1 motion; (c), (d) Poincaré map and FFT of the q_1 motion respectively; (e), (f) time trace and phase-plane portrait of the q_2 motion respectively

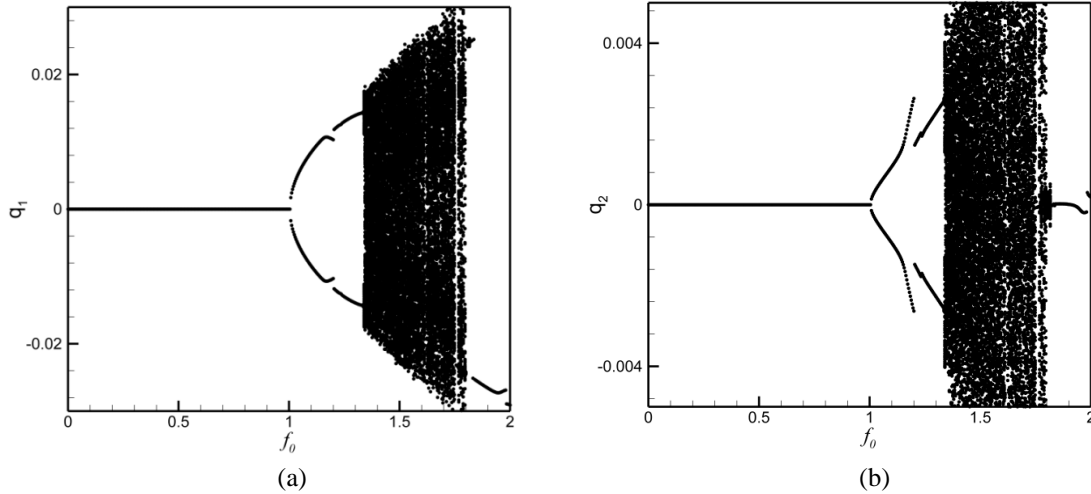


Fig. 9 Bifurcation diagrams of Poincaré points for increasing mean axial speed of the system with $f_1=0.15$

Figs. 5, 6 and 9 shows the bifurcation diagrams of Poincare sections for amplitude of speed variations of $f_1=0.05, 0.1, \text{ and } 0.15$; in these figures the mean axial speed is chosen as the bifurcation parameter. The first two generalized coordinates are only presented for brevity while twelve nonlinear ordinary differential equations are solved numerically. The other dimensionless parameters for these figures are selected as: $v_1=33.526, v_f=0.173, \mu=0.04, \alpha=1.5, \gamma=0.3, \text{ and } x_s=0.5$.

The bifurcation diagrams of the first generalized coordinates versus the mean axial speed for the case with $f_1=0.05$ are given in Figs. 5(a) and 5(b). In Fig. 5(a), the mean axial speed is increased and shows a zero response until $f_0=1.136$ where a non-zero response occurs. Although the motion resembles a period-doubling in the range of $[1.136 \text{ } 1.480]$, there are in fact two coexisting attractors and the response repeatedly jumps from one attractor to the other as the mean axial speed is increased. The motion becomes quasiperiodic at $f_0=1.484, 1.488, 1.492$ and periodic at $f_0=1.496$. As f_0 is increased a little, a sudden reduction occurs at $f_0=1.504$ and the response changes phase. As the mean axial speed is increased further, a jump occurs at $f_0=1.788$. This periodic motion continues until $f_0=2.000$.

The bifurcation diagram of the same system of Figs. 5(a) and 5(b), but with a higher value for the amplitude of the speed variations is shown in Figs. 6(a) and 6(b) -- the value for f_1 is set to 0.1. As seen in this figure, due to increased amplitude of the speed variations, the system displays more interesting and complex dynamics involving period-2 and chaotic motions in different ranges of the mean axial speed. The phase-planes and time traces of the first generalized coordinates at $f_0=1.36$ is shown in Fig. 7, illustrating a period-2 motion. Also, typical characteristics of chaotic oscillations at $f_0=1.480$ is shown in Fig. 8 through (a), (b) the time trace and phase-plane portrait of the q_1 motion, (c), (d) Poincare section, FFT of the q_1 motion, and (e), (f) the time trace and phase-plane portrait of the q_2 motion.

Increasing f_1 from 0.1 to 0.15 in Figs. 6 and 9 is generated. Due to this increased amplitude of the speed variations, the range of the chaotic region becomes wider. Comparing the dynamics of the system in Figs. 5, 6 and 9, it is observed that there is always zero response in the bifurcation diagrams; this is an interesting feature of this parametrically excited system that even though in the presence of the harmonic excitation, the zero-response still exists.

4.2 The amplitude of the speed variations as the bifurcation parameter

In this section, the amplitude of the speed variations is varied as the bifurcation parameter when the mean axial speed is fixed to 1.0 and 1.2 in Figs. 10 and 12, respectively.

As seen in Fig. 10(a), as the amplitude of the speed variations is increased, the response amplitude remains zero until $f_1 = 0.087$ where the motion becomes quasiperiodic. This quasiperiodic motion bridges to a periodic attractor, accompanied by a small jump in the response. There are two coexisting periodic attractors in the range of $[0.088 \ 0.356]$ and the response jumps from one to the other; the response is not period-2 in this range even though it looks like. As the amplitude of the speed variations is increased further, the system displays the following dynamics:

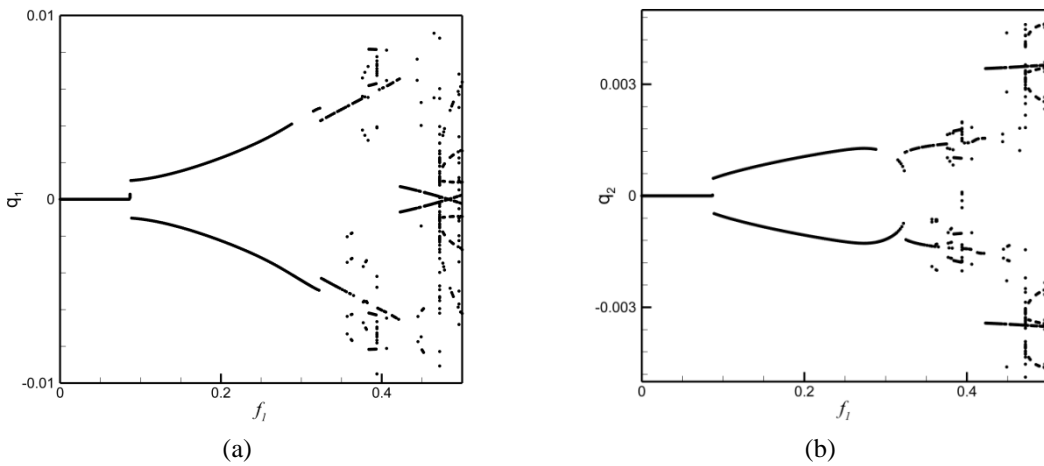


Fig. 10 Bifurcation diagrams of Poincaré points for increasing mean axial speed of the system with $f_1=0.15$

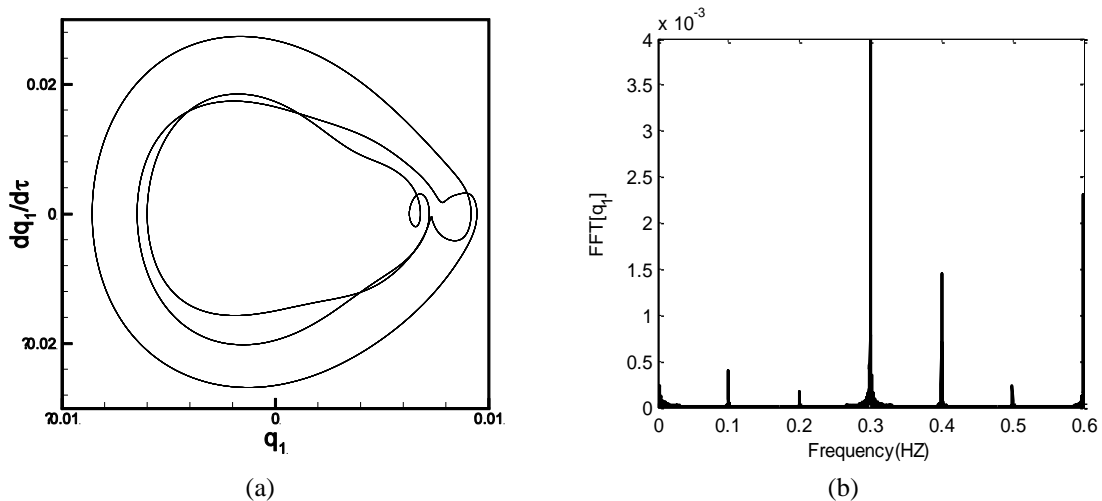


Fig. 11 Period-3 oscillation for the system of Fig. 10 at $f_1=0.379$; (a) phase-plane diagrams of the q_1 motion; (b) FFT of the q_1 motion

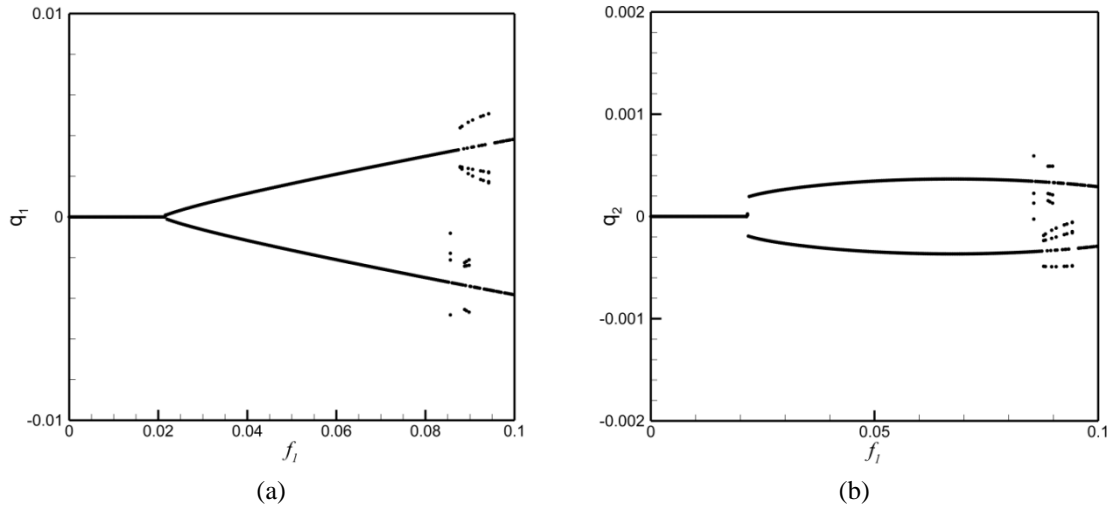


Fig. 12. Bifurcation diagrams of Poincaré points for increasing excitation amplitude on the system with $f_0=1.2$

(i) periodic, period-3, and period-4 in the range $[0.357 \ 0.383]$; (ii) period-4 in the range $[0.384 \ 0.393]$; (iii) quasiperiodic at $f_1=0.394$; (iv) periodic, period-2, period-4, and period-6 in the interval $[0.395 \ 0.500]$, except at $f_1=0.472$ where the motion is chaotic. Typical characteristics of period-3 motion at $f_1=0.379$ is shown in Fig. 11.

Fig. 12 shows the bifurcation diagram of the same system of Fig. 10, but with a higher mean axial speed (i.e., $f_0=1.2$). As seen in this figure, compared to the previous case, period-3 and period-4 motions occur at lower amplitudes of the axial speed variations. Furthermore, the non-zero solution emerges earlier.

5. Conclusions

The nonlinear resonant response as well as global complex dynamics of a hinged-hinged axially accelerating beam additionally supported by a nonlinear spring-support has been investigated in this paper using two different numerical techniques. The equation of motion was derived using Hamilton's principle and discretized via the Galerkin method, yielding a set of nonlinear ordinary differential equations. The equations were solved via the pseudo-arclength continuation technique for the system with sub-critical mean axial speed. Bifurcation diagrams of Poincaré maps were constructed using direct time integration of discretized equations of motion.

In connection with the frequency-response curves of the system, the results of this paper confirm the occurrence of the first resonance near twice the first linear natural frequency; this was predicted previously in the literature via analytical techniques such as the method of multiple timescales. In addition, results showed that there is always a trivial solution in the frequency-response of the system either possessing a three-to-one internal resonance or with no internal resonances between the first two modes. Investigation of the system dynamics showed that for both cases (i.e., with and without internal resonances) the period-doubling bifurcation exists. Apart from this bifurcation, the system with an internal resonance faces limit point and torus

bifurcations as well. Investigating the global dynamics of the system showed that the response involves periodic, period- n , and chaotic oscillations.

References

- Ahmadian, M., Nasrabadi, V. and Mohammadi, H. (2010), "Nonlinear transversal vibration of an axially moving viscoelastic string on a viscoelastic guide subjected to mono-frequency excitation", *Acta Mech.*, **214**(3), 357-373.
- Bayat, M., Pakar, I. and Bayat, M. (2013), "On the large amplitude free vibrations of axially loaded Euler-Bernoulli beams", *Steel Compos. Struct.*, **14**(1), 73-83.
- Chen, L.Q., Ding, H. and Lim, C.W. (2012), "Principal parametric resonance of axially accelerating viscoelastic beams: multi-scale analysis and differential quadrature verification", *Shock Vib.*, **19**(4), 527-543.
- Chen, L.Q. and Yang, X.D. (2005), "Steady-state response of axially moving viscoelastic beams with pulsating speed: comparison of two nonlinear models", *Int. J. Solids Struct.*, **42**(1), 37-50.
- Ding, H. and Chen, L.Q. (2010), "Galerkin methods for natural frequencies of high-speed axially moving beams", *J. Sound Vib.*, **329**(17), 3484-3494.
- Ding, H. and Chen, L. (2009), "Nonlinear dynamics of axially accelerating viscoelastic beams based on differential quadrature", *Acta Mech. Solida Sinica*, **22**(3), 267-275.
- Doedel, E.J., Champneys, A.R., Fairgrieve, T.F., Kuznetsov, Y.A., Sandstede, B. and Wang, X. (1998), *AUTO 97: Continuation and bifurcation software for ordinary differential equations (with homcont)*, Concordia University, Montreal, Canada.
- Ghayesh, M. (2012), "Stability and bifurcations of an axially moving beam with an intermediate spring support", *Nonlinear Dynam.*, **69**(1), 193-210.
- Ghayesh, M., Alijani, F. and Darabi, M. (2011), "An analytical solution for nonlinear dynamics of a viscoelastic beam-heavy mass system", *J. Mech. Sci. Tech.*, **25**(8), 1915-1923.
- Ghayesh, M.H. (2008), "Nonlinear transversal vibration and stability of an axially moving viscoelastic string supported by a partial viscoelastic guide", *J. Sound Vib.*, **314**(3-5), 757-774.
- Ghayesh, M.H. (2009), "Stability characteristics of an axially accelerating string supported by an elastic foundation", *Mech. Mach. Theory*, **44**(10), 1964-1979.
- Ghayesh, M.H. (2010), "Parametric vibrations and stability of an axially accelerating string guided by a non-linear elastic foundation", *Int. J. Nonlinear Mech.*, **45**(4), 382-394.
- Ghayesh, M.H. (2011), "Nonlinear forced dynamics of an axially moving viscoelastic beam with an internal resonance", *Int. J. Mech. Sci.*, **53**(11), 1022-1037.
- Ghayesh, M.H. (2011), "On the natural frequencies, complex mode functions, and critical speeds of axially traveling laminated beams: parametric study", *Acta Mech. Solida Sinica*, **24**(4), 373-382.
- Ghayesh, M.H., Amabili, M. and Farokhi, H. (2013), "Coupled global dynamics of an axially moving viscoelastic beam", *Int. J. Nonlinear Mech.*, **51**(0), 54-74.
- Ghayesh, M.H. and Balar, S. (2008), "Non-linear parametric vibration and stability of axially moving visco-elastic Rayleigh beams", *Int. J. Solids Struct.*, **45**(25-26), 6451-6467.
- Ghayesh, M.H. and Balar, S. (2010), "Non-linear parametric vibration and stability analysis for two dynamic models of axially moving Timoshenko beams", *Appl. Math. Model.*, **34**(10), 2850-2859.
- Ghayesh, M.H., Kazemirad, S. and Amabili, M. (2012), "Coupled longitudinal-transverse dynamics of an axially moving beam with an internal resonance", *Mech. Mach. Theory*, **52**(0), 18-34.
- Ghayesh, M.H. and Khadem, S.E. (2007), "Non-linear vibration and stability analysis of a partially

- supported conveyor belt by a distributed viscoelastic foundation”, *Struct. Eng. Mech.*, **27**(1), 17-32.
- Ghayesh, M.H. and Païdoussis, M.P. (2010), “Three-dimensional dynamics of a cantilevered pipe conveying fluid, additionally supported by an intermediate spring array”, *Int. J. Nonlinear Mech.*, **45**(5), 507-524.
- Ghayesh, M.H., Païdoussis, M.P. and Modarres-Sadeghi, Y. (2011), “Three-dimensional dynamics of a fluid-conveying cantilevered pipe fitted with an additional spring-support and an end-mass”, *J. Sound Vib.*, **330**(12), 2869-2899.
- Ghayesh, M.H., Yourdkhani, M., Balar, S. and Reid, T. (2010), “Vibrations and stability of axially traveling laminated beams”, *Appl. Math. Comput.*, **217**(2), 545-556.
- Huang, J.L., Su, R.K.L., Li, W.H. and Chen, S.H. (2011), “Stability and bifurcation of an axially moving beam tuned to three-to-one internal resonances”, *J. Sound Vib.*, **330**(3), 471-485.
- Kural, S. and Özkaya, E. (2012), “Vibrations of an axially accelerating, multiple supported flexible beam”, *Struct. Eng. Mech.*, **44**(4).
- Marynowski, K. (2004), “Non-linear vibrations of an axially moving viscoelastic web with time-dependent tension”, *Chaos Soliton. Fract.*, **21**(2), 481-490.
- Marynowski, K. and Kapitaniak, T. (2002), “Kelvin-Voigt versus Bürgers internal damping in modeling of axially moving viscoelastic web”, *Int. J. Nonlinear Mech.*, **37**(7), 1147-1161.
- Movahedian, B. (2012), “Dynamic stiffness matrix method for axially moving micro-beam”, *Int. Multiscale Mech.*, **5**(4).
- Öz, H.R. and Pakdemirli, M. (1999), “Vibrations of an axially moving beam with time-dependent velocity”, *J. Sound Vib.*, **227**(2), 239-257.
- Öz, H.R., Pakdemirli, M. and Boyacı, H. (2001), “Non-linear vibrations and stability of an axially moving beam with time-dependent velocity”, *Int. J. Nonlinear Mech.*, **36**(1), 107-115.
- Öz, H.R., Pakdemirli, M. and Özkaya, E. (1998), “Transition behaviour from string to beam for an axially accelerating material”, *J. Sound Vib.*, **215**(3), 571-576.
- Özkaya, E. and Pakdemirli, M. (2000), “Vibrations of an axially accelerating beam with small flexural stiffness”, *J. Sound Vib.*, **234**(3), 521-535.
- Pakdemirli, M. and Öz, H.R. (2008), “Infinite mode analysis and truncation to resonant modes of axially accelerated beam vibrations”, *J. Sound Vib.*, **311**(3-5), 1052-1074.
- Pakdemirli, M. and Ulsoy, A.G. (1997), “Stability analysis of an axially accelerating string”, *J. Sound Vib.*, **203**(5), 815-832.
- Pakdemirli, M., Ulsoy, A.G. and Ceranoglu, A. (1994), “Transverse vibration of an axially accelerating string”, *J. Sound Vib.*, **169**(2), 179-196.
- Pellicano, F. and Vestroni, F. (2000), “Nonlinear dynamics and bifurcations of an axially moving beam”, *J. Vib. Acoust.*, **122**(1), 21-30.
- Ravindra, B. and Zhu, W.D. (1998), “Low-dimensional chaotic response of axially accelerating continuum in the supercritical regime”, *Arch. Appl. Mech.*, **68**(3-4), 195-205.
- Riedel, C.H. and Tan, C.A. (2002), “Coupled, forced response of an axially moving strip with internal resonance”, *Int. J. Nonlinear Mech.*, **37**(1), 101-116.
- Saffari, H., Mohammadnejad, M. and Bagheripour, M.H. (2012), “Free vibration analysis of non-prismatic beams under variable axial forces”, *Struct. Eng. Mech.*, **43**(50).
- Sahebkar, S.M., Ghazavi, M.R., Khadem, S.E. and Ghayesh, M.H. (2011), “Nonlinear vibration analysis of an axially moving drillstring system with time dependent axial load and axial velocity in inclined well”, *Mech. Mach. Theory*, **46**(5), 743-760.
- Song, Z., Li, W. and Liu, G. (2012), “Stability and non-stationary vibration analysis of beams subjected to periodic axial forces using discrete singular convolution”, *Struct. Eng. Mech.*, **44**(4), 487-499.
- Suweken, G. and Van Horssen, W.T. (2003), “On the transversal vibrations of a conveyor belt with a low and time-varying velocity. Part I: the string-like case”, *J. Sound Vib.*, **264**(1), 117-133.

- Suweken, G. and Van Horssen, W.T. (2003), "On the weakly nonlinear, transversal vibrations of a conveyor belt with a low and time-varying velocity", *Nonlinear Dynam.*, **31**(2), 197-223.
- Tang, Y.Q., Chen, L.Q. and Yang, X.D. (2008), "Natural frequencies, modes and critical speeds of axially moving Timoshenko beams with different boundary conditions", *Int. J. Mech. Sci.*, **50**(10-11), 1448-1458.
- Yang, X.D. and Chen, L.Q. (2005), "Bifurcation and chaos of an axially accelerating viscoelastic beam", *Chaos Soliton. Fract.*, **23**(1), 249-258.